BIBECHANA
Vol. 20, No. 3, December 2023, 316–325

ISSN 2091-0762 (Print), 2382-5340 (Online)
Journal homepage: http://nepjol.info/index.php/BIBECHANA
Publisher:Dept. of Phys., Mahendra Morang A. M. Campus (Tribhuvan University)Biratnagar

Thermodynamic, structural and surface properties of rare earth metallic alloys: Au-La liquid system

S. K. Yadav*
Department of Physics, Mahendra Morang Adarsh Multiple Campus Biratnagar, Nepal.
*Corresponding author: Email: sashit.yadav@mmamc.tu.edu.np

Abstract

A complete information related to the mixing behaviours of Au alloyed with rare earth metals or lanthanides is very scarce. Therefore, an attempt has been made in this work to compute and study the temperature and concentration dependent thermodynamic, structural and surface properties of Au-La liquid alloy using different theoretical approaches. The thermodynamic properties, such as excess Gibbs free energy of mixing, enthalpy of mixing, excess entropy of mixing and activity of the system were computed using available coefficients of interaction energy parameters in the framework of Redlich-Kister polynomial. Taking these as reference values, model parameters for quasi-lattice model were optimised at 1473 K. The model parameters were then determined at higher temperatures assuming them to be linear temperature-dependent. The thermodynamic and structural properties were then computed in the temperature range 1473 K-1773 K. The surface properties of the system were computed using Bulter's model using determined values of partial excess Gibbs free energy of its components. Present investigations revealed that the compound forming tendency of the system gradually decreased with increase in temperature of the system.

Keywords
Ordering energy, hetero-coordinating nature, segregating nature, surface segregation, surface tension.

Article information
Manuscript received: March 10, 2023; Accepted: March 25, 2023
DOI https://doi.org/10.3126/bibechana.v20i3.59896

1 Introduction

Development of lead free solders has been a great task for the researchers working in the field of materials design and fabrication. One of the most promising alternative for the purpose has been found to be the use of Sn-based alloys, more precisely Sn-Ag-Cu ternary alloys. Addition of small amount of rare earth (RE) elements to these alloys, increases the mechanical behaviour, creep-fatigue resistance and wetting properties [1–4]. In due course, knowledge related to the mixing behaviours of RE-based liquid alloys are important. But a very few information regarding the thermo-physical properties of metallic alloys having RE metals, also called lanthanide, as ingredient is available to date. In order to develop the thermodynamic database of RE-based liquid alloy, the thermodynamic and structural properties of Au-La liquid alloy was studied in the previous work [5]. To further enhance the procedure, the mixing properties of Au-La liquid alloy have been computed and studied at different

temperatures in the present work.

Dong et al. in 2011 [6] have summarized the details of literature associated with the works carried out by different researchers to assess the mixing properties of Au-La alloy. In their work, phase relations in Au-La and Au-Er alloys have been thermodynamically studies using CALPHAD technique incorporated with the ab initio calculations. They calculated enthalpy of mixing of the system at 1473 K and compared them with the experimental values of Fitzner et al. [7]. Further, they presented the self consistent parameters of Redlich-Kister polynomial [8] for the excess Gibbs free energy of mixing for different phases present in the alloy. They calculated the existence of different stable phases, such as $AuLa_2$, $AuLa$, Au_2La, $Au_{51}La_{14}$ and Au_6La. These results were found to be in good agreement with those obtained by Massalski [9], except for the reaction temperature and composition involving the constitution of Au_2La and $Au_{51}La_{14}$ phases. They found the reaction temperature to be 75 K higher and close to $x_{\mathrm{Au}} = 0.04$ than observed by Massalski. In the knowledge of the author of this work, the complete description of the mixing properties of the system is lacking to date.

Therefore, an attempt has been made in this work to study and explain the thermodynamic, structural and surface properties of the liquid alloy at different temperatures. In thermodynamic properties, such as excess Gibbs free energy of mixing (ΔG_M^{xs}), enthalpy of mixing (ΔH_M), entropy of mixing (ΔS_M^{xs}) and activity (a_i; $i = \mathrm{Au}, \mathrm{La}$) were computed using modeling equations of quasi-lattice model. In the same frame, the structural properties, such as concentration fluctuation in long wavelength limit ($S_{\mathrm{CC}}(0)$), Warren-Cowley short range order parameter (α_1) and ratio of mutual to intrinsic diffusion coefficients (D_M/D_{id}) were calculated. The surface tension and surface concentrations of the system were calculated using Butler's model [10–13].

2 Formulations

2.1 Quasi–lattice model

This theoretical approach assumes that when two elements A and B are mixed in liquid state, the formation of the complex of the type $\mathrm{A}_\mu\mathrm{B}_\nu$ takes place. The values of $_\mu$ and $_\nu$ depend upon stiochiometric compositions at which the stable phase is present and are determined from the phase diagram of the system. In this work, the existence of the complex Au_2La [6, 7] was considered as energetically favoured . In this regard, the expression for excess Gibbs free energy of mixing (ΔG_M^{xs}) can be given as [14–16]

$$\Delta G_M^{\mathrm{xs}} = N[\Phi\omega + \Phi_{AB}\omega_{AB} + \Phi_{AA}\omega_{AA}] \quad (1)$$

where ω, ω_{AB} and ω_{AA} are the interaction energy or model parameters. They are assumed to be temperature-dependent but concentration independent. Φ, Φ_{AB} and Φ_{AA} are the simple polynomials in x_1 and x_2, such that $x_1 + x_2 = 1$. Φ, Φ_{AB} and Φ_{AA} are expressed as [14–16]

$$\begin{aligned} \Phi &= x_1 x_2 \\ \Phi_{AB} &= \frac{x_1}{6} + x_1^2 - \frac{5x_1^3}{3} + \frac{x_1^4}{2} \\ \Phi_{AA} &= -\frac{x_1}{4} + \frac{x_1^2}{2} - \frac{x_1^4}{4} \end{aligned} \quad (2)$$

ΔG_M^{xs} can be expressed in terms of Gibbs free energy of mixing (ΔG_M) as

$$\Delta G_M = \Delta G_M^{\mathrm{xs}} + RT[x_1 \ln x_1 + x_2 \ln x_2] \quad (3)$$

where R (in J/(mol.K) is the real gas constant and T (in K) is the absolute temperature. The excess entropy of mixing (S_M^{xs}) is related to ΔG_M^{xs} as

$$\Delta S_M^{\mathrm{xs}} = -\left(\frac{\partial \Delta G_M^{\mathrm{xs}}}{\partial T}\right)_P \quad (4)$$

From Equations (1) and (4), one can obtain

$$\Delta S_M^{\mathrm{xs}} = -N\left[\frac{\partial \Delta\omega}{\partial T}\Phi + \frac{\partial \Delta\omega_{AB}}{\partial T}\Phi_{AB} + \frac{\partial \Delta\omega_{AA}}{\partial T}\Phi_{AA}\right] \quad (5)$$

Herein, $\frac{\partial \Delta\omega}{\partial T}$, $\frac{\partial \Delta\omega_{AB}}{\partial T}$ and $\frac{\partial \Delta\omega_{AA}}{\partial T}$ are the temperature derivative terms of interaction energy parameters.

The enthalpy of mixing (ΔH_M) can be related to ΔG_M^{xs} and ΔS_M^{xs} by the well known thermodynamic expression as

$$\Delta H_M = \Delta G_M^{\mathrm{xs}} + T\Delta S_M^{\mathrm{xs}} \quad (6)$$

Using Equation (4) in Equation (6), yields

$$\Delta H_M = \Delta G_M^{\mathrm{xs}} - T\left(\frac{\partial \Delta G_M^{\mathrm{xs}}}{\partial T}\right)_P \quad (7)$$

The activity of component i (a_i; $i = Au, La$) in the binary solution can be expressed in terms of ΔG_M as

$$RT \ln a_i = \Delta G_M + (1 - x_i)\left(\frac{\partial \Delta G_M}{\partial x_i}\right)_{T,P,N} \quad (8)$$

Using Equations (1) and (3) in Equation (8), one can obtain the expression for $\left(\frac{\partial \Delta G_M}{\partial x_i}\right)_{T,P,N}$ as

$$\left(\frac{\partial \Delta G_M}{\partial x_i}\right)_{T,P,N} = \Delta\omega\Phi^{'} + \Delta\omega_{AB}\Phi_{AB}{}^{'} + \Delta\omega_{AA}\Phi^{'}_{AA} + \ln\left(\frac{x_i}{1-x_i}\right) \quad (9)$$

where $\Phi^{'}$ and $\Phi^{'}_{ij}$ are the first order derivatives of respective parameters (in Equation (2)) with respect to concentration of i^{th} element.

To study and understand the arrangement of atoms at atomic level in the initial melt, the structural functions have become an essential tool. Among them, the expression for concentration fluctuation in long wavelength limit ($S_{CC}(0)$) is expressed as [17–20]

$$S_{CC}(0) = RT\left(\frac{\partial^2 G_M}{\partial x_1^2}\right)^{-1}_{T,P,N} = RT\left(\frac{\partial^2 G_M}{\partial x_2^2}\right)^{-1}_{T,P,N} \quad (10)$$

Using Equations (1) and (3) in Equation (10), yields

$$S_{\text{CC}}(0) = x_1x_2[1 + x_1x_2RT(\Delta\omega\Phi'' + \Delta\omega_{AB}\Phi^{''}_{AB} + \Delta\omega_{AA}\Phi^{''}_{AA})]^{-1} \quad (11)$$

where ϕ'' and $\phi_{ij}{}''$ are the second order derivatives of respective parameters with respect to concentration (x_i) and can be obtained from Equation (2). The ideal values of $S_{\text{CC}}(0)$ is obtained by the following relation

$$S^{id}_{\text{CC}}(0) = x_1x_2 \quad (12)$$

The structural functions, Warren-Cowley short range–order parameter (α_1) and the ratio of mutual to intrinsic diffusion coefficients (D_M/D_{id}) can be expressed in terms of $S_{\text{CC}}(0)$ as [13, 15, 18, 21]

$$\alpha_1 = \frac{S-1}{[S(Z-1)+1]} \quad (13)$$

with

$$S = \frac{S_{\text{CC}}(0)}{S^{id}_{\text{CC}}(0)} \quad (14)$$

and

$$\frac{D_M}{D_{\text{id}}} = \frac{S^{id}_{\text{CC}}(0)}{S_{\text{CC}}(0)} \quad (15)$$

2.2 Redlich-Kister (R-K) polynomial

R-K polynomial is used to model the temperature-dependent thermodynamic properties of liquid alloys. It is extensively used as modeling equations in theoretical calculations, software based computations and experimental measurements [6, 8]. In this approach, ΔG^{xs}_M is expressed as [5, 6, 8, 22]

$$\Delta G^{\text{xs}}_M = x_1x_2\sum_{q=0}^{n} L_q(x_1-x_2)^q \quad (16)$$

where L_q are the linear T–dependent coefficients or interaction energy parameters of R-K polynomial. They are expressed in the form $L_q = a_q + b_qT$, where a_q (in J/mol) are contributions due to ΔH_M and b_q (in J/mol-K) are contributions of ΔS^{xs}_M to ΔG^{xs}_M equivalent to Equations 6.
The partial excess Gibbs free energy (ΔG^{xs}_i) of the component i in the binary liquid alloy can be given as [22]

$$\Delta G^{\text{xs}}_i = \Delta G^{\text{xs}}_M + (1-x_i)\left(\frac{\partial \Delta G^{\text{xs}}_M}{\partial x_i} - \frac{\partial \Delta G^{\text{xs}}_M}{\partial (1-x_i)}\right) \quad (17)$$

The activity coefficient of component i in the binary solution is related to ΔG^{xs}_i as

$$RT\ln\gamma_i = \Delta G^{\text{xs}}_i \quad (18)$$

After the computations of γ_i, the activity of component i can be obtained by the relation

$$a_i = x_i\gamma_i \quad (19)$$

The values of S^{xs}_M and H_M can be obtained using Equations (4), (7) and (16). Using Equations (10) and (16), $S_{CC}(0)$ for this system having $q = 0, 1$ can be obtained as [5, 23]

$$S_{\text{CC}}(0) = RT[-2L_0 + (-12x_1+6)L_1 + \frac{RT}{x_1(1-x_1)}]^{-1} \quad (20)$$

The values of other structural functions in this framework can also be obtained using Equations (13-15).

2.3 Butler model

The surface properties, surface tension (σ) and surface concentrations (x^S_i) of the system have been calculated using Butler model. According to this model, σ for binary liquid solution can be given as [10–13]

$$\sigma = \sigma_1 + \frac{RT}{A_1}\ln\frac{x_1^S}{x_1^b} + \frac{\Delta G^{\text{xs}}_{1,S} - \Delta G^{\text{xs}}_{1,b}}{A_1}$$
$$= \sigma_2 + \frac{RT}{A_2}\ln\frac{x_2^S}{x_2^b} + \frac{\Delta G^{\text{xs}}_{2,S} - \Delta G^{\text{xs}}_{2,b}}{A_1} \quad (21)$$

where σ_i is the surface tension, A_i is molar surface area, x_i^S is the surface concentration, x_i^b is the bulk concentration, $\Delta G^{\text{xs}}_{i,S}$ is the molar surface partial excess Gibbs free energy and $\Delta G^{\text{xs}}_{i,b}$ is the molar bulk partial excess Gibbs free energy for the component i of the liquid mixture at the melting temperature of the alloy. $\Delta G^{\text{xs}}_{i,S}$ and $\Delta G^{\text{xs}}_{i,b}$ related by the relation

$$\Delta G^{\text{xs}}_{i,S} = \beta \Delta G^{\text{xs}}_{i,b} \quad (22)$$

where $\beta = 0.8181$ [11,13] for simple liquid metals. The molar surface area (A_i) of component i in the liquid mixture can be calculated using the relation

$$A_i = f N_A^{\frac{1}{3}} V_i^{\frac{2}{3}} \quad (23)$$

where N_A is the Avogadro's number and $V_i (= \frac{m_i}{\rho_i})$ is the molar volume of element i in the liquid mixture. The values of σ_i and V_i are calculated with the help of the following relations [11,24]

$$\sigma_i = \sigma_i^0 + \frac{d\sigma}{dT}(T - T_0) \quad (24)$$

and

$$V_i = V_i^0[1 + +\lambda_i(T - T_0)] \quad (25)$$

where σ_i^0 is the surface tension, V_i^0 is the molar volume and λ_i [11,24] is the temperature coefficient of volume expansion for i^{th} component at its melting temperature (T_0).

3 Results and Discussion

3.1 Thermodynamic properties

The self-consistent parameters for excess Gibbs free energy of mixing (ΔG^{xs}_M) of Au–La liquid alloy were taken from Dong et al. [6] (Table 1). These parameters were used to calculate ΔG^{xs}_M of the system at 1473 K in the frame work of R-K polynomial [8] (Equation (16)). The values so computed were considered as reference data and then quasi–lattice model was employed to determine the model fit parameters using Equations (1-3). The best fit values of the model parameters were estimated assuming the existence of Au_2La complex and are presented in Table 1.

Table 1: Interaction energy parameters for ΔG^{xs}_M of Au–La liquid alloy

Parameters [J/mol]	Reference
$L_0 = -254446.24 + 6.00025 * T$ $L_1 = -85046.07 + 2.89377 * T$	[6]
$\Delta\omega = -264279.94476 + 8.97912 * dT$ $\Delta\omega_{AB} = -3042.03606 + 0.083140 * dT$ $\Delta\omega_{AA} = -345964.24650 + 1.66280 * dT$	This work

The determined values of model parameters $\Delta\omega$, $\Delta\omega_{AB}$ and $\Delta\omega_{AA}$ were found to have negative values (Table 1). Among them, $\Delta\omega$ is called ordering energy parameter and its value was estimated to be -264279.94476 indicating the system to be strongly interacting in nature. The value of ΔG^{xs}_M was computed at 1473 K using the parameters from Table 1 and Equations (1-3). The compositional dependence of ΔG^{xs}_M of the this work along with the values computed using the parameters of Dong et al. are displayed in Figure 1.

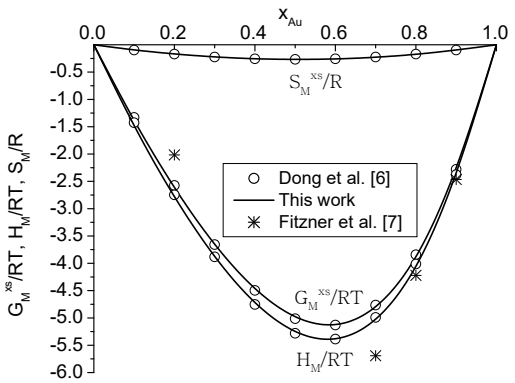

Figure 1: Compositional dependence of $\Delta G^{\text{xs}}_M/RT$, $\Delta H_M/RT$ and $\Delta S^{\text{xs}}_M/R$ of Au–La liquid alloy at 1473 K.

The computed values of ΔG^{xs}_M were found to be in consistent with each other at compositions thereby validating the present optimisation procedure (Figure 1). The maximum negative value of $\Delta G^{\text{xs}}_M = -5.12014$RT (this work) and $\Delta G^{\text{xs}}_M = -5.12991$RT (Dong et al.) [6] at $x_{\text{Au}} = 0.6$. The high negative value of $\Delta G^{\text{xs}}_M/RT$ indicates the system to be strongly interacting in nature at its melting temperature, 1473 K. Moreover, the system is found to be asymmetric with respect to ΔG^{xs}_M.

The enthalpy of mixing ($\Delta H_M/RT$) and excess entropy of mixing $\Delta S^{\text{xs}}_M/R$ of the system were calculated with the help of parameters from Table 1 and Equations (4-7). These computed values are portrayed as a function of composition in Figure 1.

The extremum negative value of $\Delta H_M/RT = -5.37922$RT (this work) and $\Delta H_M/RT = -5.38665$RT (Dong et al. [6]) at $x_{\mathrm{Au}} = 0.6$. The high negative value of H_M/RT corresponds the strong association between Au and La in the assumed complex at 1473 K. Further, the computed values of $\Delta H_M/RT$ of this work and those of Dong et al. were consistent with each other and the system is found to be asymmetric with respect this physical function. The values of $\Delta H_M/RT$ were also found to be in agreement with the experimental values of Fitzner et al. [7] at higher compositions of Au. Likewise, the maximum negative value of $\Delta S_M^{\mathrm{xs}} = -0.26781$R (this work) and $\Delta S_M^{\mathrm{xs}} = -0.26744$R (Dong et al.) at $x_{\mathrm{Au}} = 0.5$. The Au-La liquid alloy is found to be symmetric with respect to ΔS_M^{xs}. Thus, the above theoretical investigations reveal that the model parameters determined in the frame work of quasi-lattice model are fruitful in explaining the thermodynamic properties of the system.

To further validate the present optimisation process, the activity of the system was computed using the same determined model parameters. The activities of the individual atoms (a_{Au} and a_{La}) of the initial melt were calculated on the basis of R-K polynomial (Equations (16-19)) and quasi-lattice model (Equations (8 and 9)) using the parameters from Table 1. The calculated and ideal values of a_{Au} and a_{La} are plotted as a function of concentration in Figure 2.

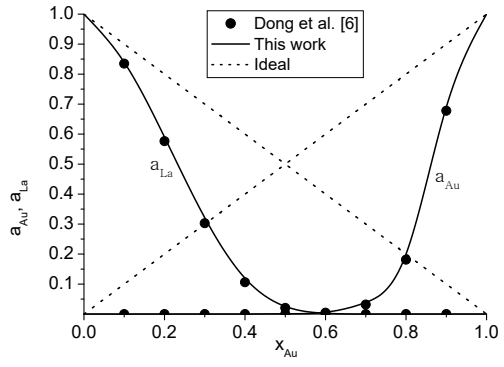

Figure 2: Computed values of a_{Au} and a_{La} versus concentration of Au (x_{Au}) of Au–La liquid alloy at 1473 K.

The computed values of a_{Au} and a_{La} were found to be much less than their respective ideal values at all compositions indicating the system to be strongly interacting in nature. Both of these values, computed using the parameters of present work and Dong et al., were found to be consistent with each other at all concentrations (Figure 2). Thus, it can be stated that the preferred model is capable of explaining the thermodynamic functions and reproducing the activity of the system. Therefore, these model parameters were considered for the computations of structural and surface properties.

In thermodynamic properties, ΔG_M^{xs}, ΔH_M and $a_i; i = \mathrm{Au}, \mathrm{La}$ were computed at different temperatures assuming the model parameters of quasi-lattice model to be linear temperature-dependent. The model parameters $\Delta\omega$, $\Delta\omega_{AB}$ and $\Delta\omega_{AA}$ in correlation with their respective temperature derivatives terms $\partial\Delta\omega/\partial T$, $\partial\Delta\omega_{AB}/\partial T$ and $\partial\Delta\omega_{AA}/\partial T$ can be expressed as [5, 13]

$$\Delta\omega(T) = \Delta\omega(T_0) + \frac{\partial\Delta\omega}{\partial T}(T - T_0) \qquad (26)$$

$$\Delta\omega_{ij}(T) = \Delta\omega_{ij}(T_0) + \frac{\partial\Delta\omega_{ij}}{\partial T}(T - T_0) \qquad (27)$$

where T_0 (= 1473 K) is the melting temperature of the system and T is the temperature of interest at which thermodynamic properties are to be calculated. The determined values of temperature-dependent model parameters for this liquid alloy are portrayed in Table 1.

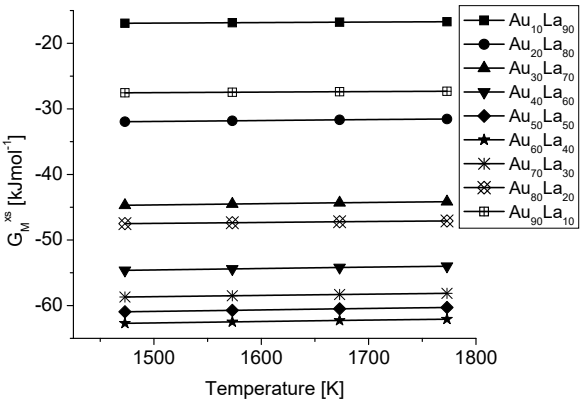

Figure 3: Temperature dependence of excess Gibbs free energy of mixing (ΔG_M^{xs}) for Au–La liquid alloy.

The values of ΔG_M^{xs} were computed using Equations (1 and 2), ΔH_M were computed using Equations (1 and 7) and a_i were computed using Equations (17-19) at different temperatures with the aid of parameters in Table 1. The temperature variation of ΔG_M^{xs} and ΔH_M at fixed composition ratios of Au and La are presented in Figures 3 and 4. The compositional dependence of a_i at different temperatures are plotted in Figures 5 and 6.

The negative values of ΔG_M^{xs} and ΔH_M decreased linearly with increased in temperature of the system.

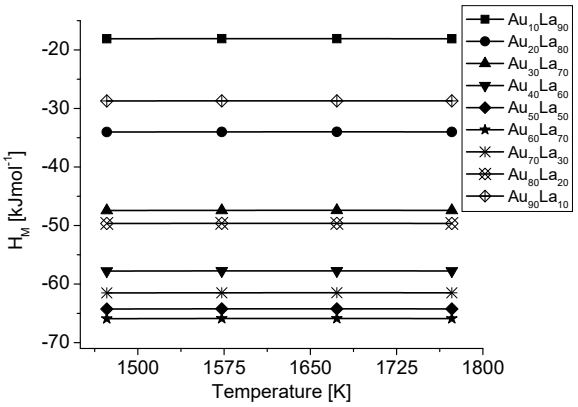

Figure 4: Variation of ΔH_M with temperature of Au–La liquid alloy.

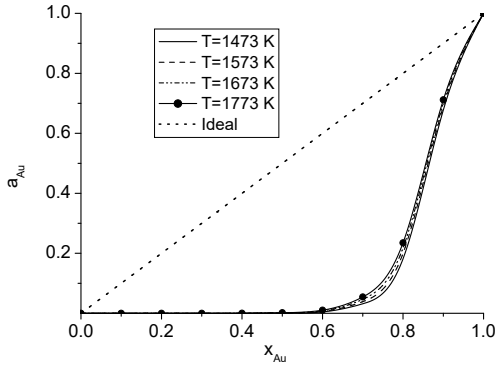

Figure 5: Activity of Au (a_{Au}) versus x_{Au} in temperature range 1474–1773 K.

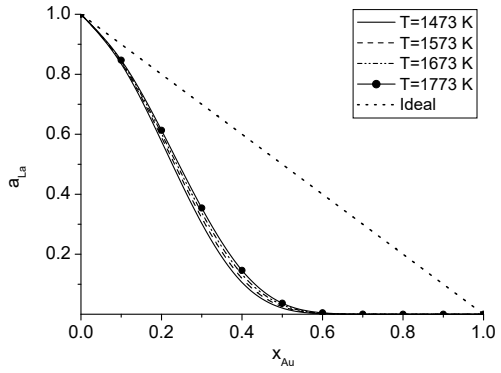

Figure 6: Compositional dependence of activity of La (a_{La}) at different temperatures.

These results revealed the decrease in the complex formation tendency or strength of interaction between the monomers. Indeed, the activities of Au and La gradually increased with increase in temperature. The deviation of a_i from ideal values gradually decreased with increase in temperature indicating the decrease in mixing tendency of the system (Figures 5 and 6).

3.2 Structural properties

The information related to the local arrangement of atoms in the initial melt can be obtained form the knowledge of structural functions. In structural functions, concentration fluctuation in long wavelength limit ($S_{\mathrm{CC}}(0)$), Warren-Cowley short range order parameter (α_1) and ratio of mutual to intrinsic diffusion coefficients (D_M/D_{id}) were computed in the frame work of quasi-lattice model using Equations (10-15) and parameters from Table 1. Likewise, Equations (12-15) and (20) were used to calculate these values on the basis of R-K polynomial with the aid of parameters of Dong et al. (Table 1). The compositional dependence of $S_{\mathrm{CC}}(0)$, α_1 and D_M/D_{id} are plotted in Figures 7 and 8.

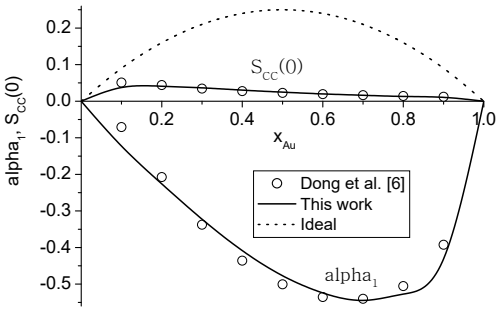

Figure 7: Computed values of $S_{\mathrm{CC}}(0)$ and α_1 of Au–La liquid alloy at 1473 K.

At a temperature and concentration, if $S_{\mathrm{CC}}(0) < S_{\mathrm{CC}}^{\mathrm{id}}(0)$, $\alpha_1 < 0$ and $D_M/D_{\mathrm{id}} > 1$, then complex formation tendency or hetero-coordinating tendency in the alloy is expected. At the same constraints, if $S_{\mathrm{CC}}(0) > S_{\mathrm{CC}}^{\mathrm{id}}(0)$, $\alpha_1 > 0$ and $D_M/D_{\mathrm{id}} < 1$, then self association among the atoms of alloy or homo-coordinating tendency is expected. The computed values of $S_{\mathrm{CC}}(0)$ showed negative deviation with respect to its ideal values in the entire concentration range indicating the system to be ordering in nature. This finding is further supported by the negative values of α_1 and $D_M/D_{\mathrm{id}} > 1$ (Figures 7 and 8). Moreover, the values of $S_{\mathrm{CC}}(0)$ and α_1 computed using the parameters of this work and Dong et al. [6] were found to be consistent with each other at all concentrations.

Following the similar procedure as mentioned above, the values of $S_{CC}(0)$, α_1 and $D_M/D_{id} > 1$ were computed in the temperature range 1473-1773 K. The compositional and temperature dependence of these functions are displayed in Figures 9-11.

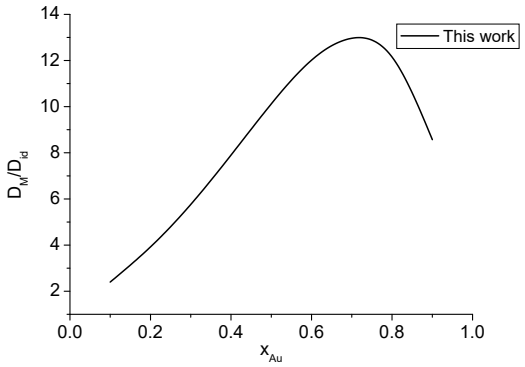

Figure 8: Computed values of D_M/D_{id} versus x_{Au} of Au–La liquid alloy at 1473 K.

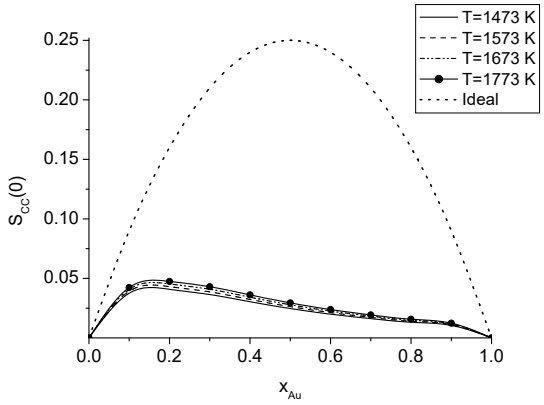

Figure 9: $S_{CC}(0)$ versus x_{Au} of Au–La liquid alloy at different temperatures.

The computed values of $S_{CC}(0)$ gradually increased and got closure to its ideal values with the rise in temperature of the system above its melting temperature (Figure 9). At equiatomic composition ($x_{Au} = 0.5$), the deviation of $S_{CC}(0)$ from $S^{id}_{CC}(0)$ were found to be -0.22529, -0.22370, -0.22211 and -0.22054 at 1473 K, 1573 K, 1673 K and 1773 K respectively. These decrease in negative deviations correspond the decrease in in compound forming tendency in the initial melt at high temperatures.

This result is further supported by the decrease in negative values of α_1 and decrease in positive values of D_M/D_{id} with increase in temperature of the system (Figures 10 and 11). At $x_{Au} = 0.5$, the computed values of α_1 were found to be -0.47692, -0.45959, -0.44331 and -0.42814 and those of D_M/D_{id} were computed to be 10.11753, 9.50450, 8.96344 and 8.48676 at 1473 K, 1573 K, 1673 K and 1773 K respectively. These results further stands in favour of those revealed by $S_{CC}(0)$. Thus, the results obtained from the investigations of structural functions are in accordance with those indicated by the thermodynamic functions in the above section.

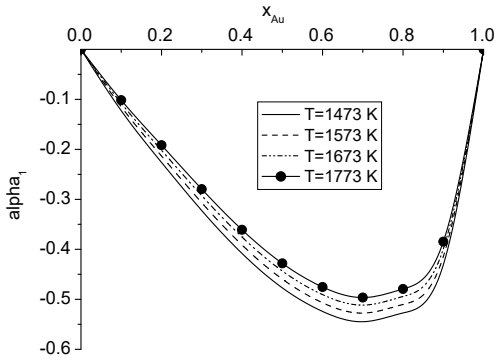

Figure 10: α_1 versus x_{Au} of Au–La liquid alloy at different temperatures.

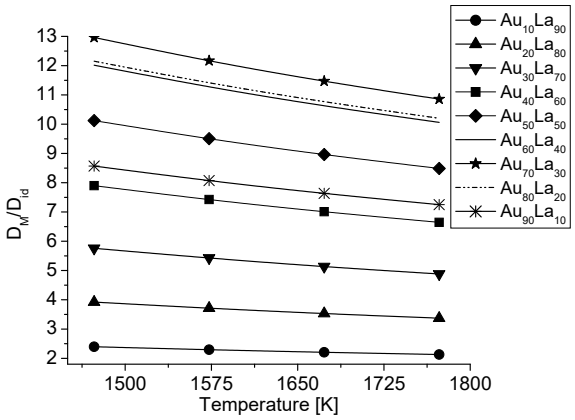

Figure 11: Computed values of D_M/D_{id} of Au–La liquid alloy at different temperatures.

3.3 Surface properties

In surface properties, surface tension (σ) and extent of surface segregation (surface concentrations, x^s_i) were computed in the frame work of Butler model [10, 24] using Equations (26-25) and parameters from Table 2. The compositional dependence of x^s_i and σ are portrayed in Figures 12 and 13 respectively.

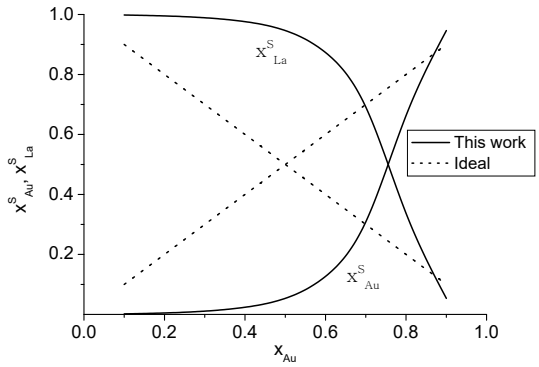

Figure 12: Computed values of x^S_{Au} and x^S_{La} versus x_{Au} of Au–La liquid alloy at 1473 K.

The surface concentration of La (x^S_{La}) showed positive deviation whereas that of Au (x^S_{Au}) showed negative deviation from their respective ideal values in the concentration range $x^S_{\mathrm{Au}} < 0.9$ (Figure 12). Among the two components, La has the lower surface tension ($\sigma_{\mathrm{La}} = 0.63360$ N/m) and that of Au is higher ($\sigma_{\mathrm{Au}} = 1.13475$ N/m) at 1473 K, melting temperature of the system. Therefore, La segregated in the surface phase and Au remained in the bulk phase of the initial melt in the range $x^S_{\mathrm{Au}} < 0.9$. x^S_{Au} gradually increased and x^S_{La} gradually decreased with the increase in the bulk concentration of Au (x_{Au}). They exceed their respective ideal values beyond $x^S_{\mathrm{Au}} > 0.9$ indicating exchange of their positions in the two phases of melt. The computed values σ of the system gradually increased with increased in the bulk concentration of Au. It showed negative deviation from its ideal value beyond $x_{\mathrm{Au}} < 0.6$ while showed positive deviation in the remaining range (Figure 13).

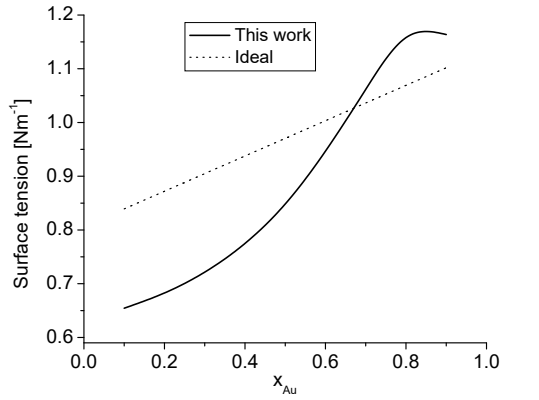

Figure 13: Compositional dependence of σ of Au–La liquid alloy at 1473 K.

Table 2: Input parameters for surface tension [25]

Atom	T_0 (K)	ρ_0 (kg/m^3)	$\partial\rho/\partial T$ (kg/m^{3}K)	σ_0 (N/m)	$\partial\sigma/\partial T$ (N/mK)
Au	1336	17360	-1.50	1.169	-0.00025
La	1203	5955	-0.24	0.720	-0.00032

The surface tension and surface concentrations of the components of the system were also calculated at different temperatures with the aid of Equations (26-25) and parameters from Table 2. The compositional and temperature dependence of estimated values are presented in Figures 14-16.

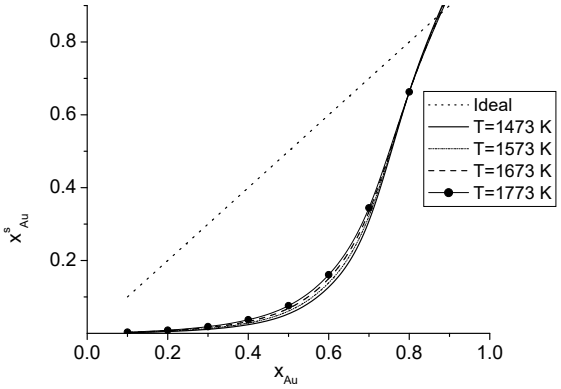

Figure 14: Computed values of x^S_{Au} versus x_{Au} of Au–La liquid alloy at different temperatures.

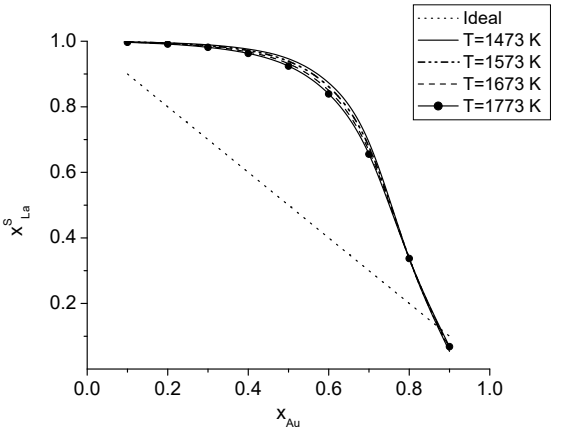

Figure 15: Computed values of x^S_{La} versus x_{Au} of Au–La liquid alloy at different temperatures.

The surface concentrations of Au gradually increased and those of La gradually decreased with increase in temperature of the liquid mixture. The negative deviations of x_{Au} and positive deviation of x_{La} from their respective ideal values eventually decreased at elevated temperature (Figure 14 and 15). Therefore, Au atoms move from bulk to surface phase while those of La moves from surface

to bulk phase to maintain the equilibrium condition in the liquid. Moreover, the surface tension of the mixture gradually decreased linearly with the increase in temperature beyond its melting temperature (Figure 16). These results are as expected since the cohesive force between the components of the liquid mixture gradually decreases with the increase in temperature.

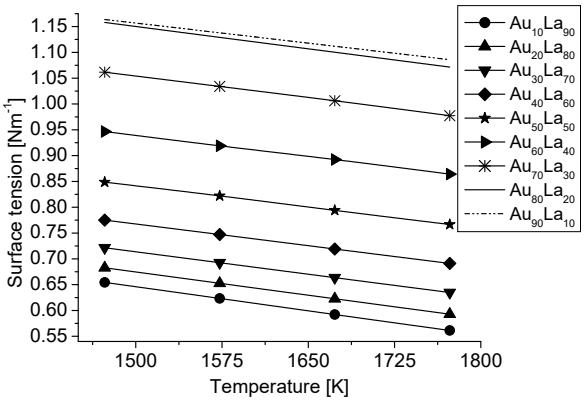

Figure 16: Variation of σ with temperature of Au–La liquid alloy.

4 Conclusions

The preferred theoretical models, quasi-lattice and Butler's models, successfully explained the compositional and temperature dependence of thermodynamic, structural and surface properties of Au-La liquid alloy. The system was found to be the most interacting at its melting temperature whereas this tendency gradually decreased with increase in temperature. The surface tension of the system decreased linearly at elevated temperatures. The results obtained from the theoretical investigations of thermodynamic, structural and surface properties were in accordance with each other.

References

[1] D. Q. Yu, J. Zhao, and L. Wang. Improvement on the microstructure stability, mechanical and wetting properties of Sn–Ag–Cu lead-free solder with the addition of rare earth elements. *Journal of alloys and compounds*, 376(1-2):170–175, 2004.

[2] WeiMin Xiao, YaoWu Shi, GuangChen Xu, Ren Ren, Fu Guo, ZhiDong Xia, and YongPing Lei. Effect of rare earth on mechanical creep–fatigue property of SnAgCu solder joint. *Journal of alloys and compounds*, 472(1-2):198–202, 2009.

[3] Z. G. Chen, Y. W. Shi, Z. D. Xia, and Y. F. Yan. Study on the microstructure of a novel lead-free solder alloy SnAgCu-RE and its soldered joints. *Journal of electronic materials*, 31:1122–1128, 2002.

[4] C. M. L. Wu, D. Q. Yu, C. M. T. Law, and L. Wang. Improvements of microstructure, wettability, tensile and creep strength of eutectic Sn–Ag alloy by doping with rare-earth elements. *Journal of materials research*, 17(12):3146–3154, 2002.

[5] S. K. Yadav. Assessment of Thermodynamic and Structural Properties of Al–Er liquid Alloy at Different Temperatures. *The Journal of Knowledge and Innovation*, pages 66–74, 2023.

[6] H. Q. Dong, X. M. Tao, H. S. Liu, T. Laurila, and M. Paulastro-Kröckel. Thermodynamic assessment of Au–La and Au–Er binary systems. *Journal of alloys and compounds*, 509(13):4439–4444, 2011.

[7] K. Fitzner, W. G. Jung, and O. J. Kleppa. Thermochemistry of binary alloys of transition metals: the Me-Sc, Me-Y, and Me-La (Me= Ag, Au) systems. *Metallurgical Transactions A*, 22:1103–1111, 1991.

[8] O. Redlich and A. T. Kister. Algebraic representation of thermodynamic properties and the classification of solutions. *Industrial & Engineering Chemistry*, 40(2):345–348, 1948.

[9] T. B. Massalski. Binary alloy phase diagrams. *ASM International*, 1990.

[10] J. A. V. Butler. The thermodynamics of the surfaces of solutions. *Proceedings of the Royal Society of London. Series A, Containing Papers of a Mathematical and Physical Character*, 135(827):348–375, 1932.

[11] George Kaptay. A unified model for the cohesive enthalpy, critical temperature, surface tension and volume thermal expansion coefficient of liquid metals of bcc, fcc and hcp crystals. *Materials Science and Engineering: A*, 495(1-2):19–26, 2008.

[12] George Kaptay. Partial surface tension of components of a solution. *Langmuir*, 31(21):5796–5804, 2015.

[13] S. K. Yadav, M. Gautam, and D. Adhikari. Mixing properties of Cu–Mg liquid alloy. *AIP Advances*, 10(12):125320, 2020.

[14] A. B. Bhatia and R. N. Singh. A quasi–lattice theory for compound forming molten alloys. *Physics and Chemistry of Liquids an International Journal*, 13(3):177–190, 1984.

[15] D. Adhikari, S. K. Yadav, and L. N. Jha. Thermo-physical properties of Mg-Tl melt. *Journal of Basic and Applied Research International*, 9:103–110, 2015.

[16] S. K. Yadav, S. Lamichhane, L. N. Jha, N. P. Adhikari, and D. Adhikari. Mixing behaviour of Ni–Al melt at 1873 K. *Physics and Chemistry of Liquids*, 54(3):370–383, 2016.

[17] A. B. Bhatia and W. H. Hargrove. Concentration fluctuations and thermodynamic properties of some compound forming binary molten systems. *Physical Review B*, 10(8):3186, 1974.

[18] S. K. Yadav, L. N. Jha, and D. Adhikari. Thermodynamic and structural properties of Bi-based liquid alloys. *Physica B: Condensed Matter*, 475:40–47, 2015.

[19] S. K. Yadav, L. N. Jha, and D. Adhikari. Segregating to ordering transformation in In–Sn melt. *Physics and Chemistry of Liquids*, 53(4):443–454, 2015.

[20] S. K. Yadav, L. N. Jha, and D. Adhikari. Thermodynamic, structural, transport and surface properties of Pb-Tl liquid alloy. *Bibechana*, 13:100–113, 2016.

[21] D. Adhikari, S. K. Yadav, and L. N. Jha. Thermo-physical properties of Al–Fe melt. *Journal of the Chinese Advanced Materials Society*, 2(3):149–158, 2014.

[22] S. K. Yadav, U. Mehta, and D. Adhikari. Optimization of thermodynamic and surface properties of ternary Ti–Al–Si alloy and its subbinary alloys in molten state. *Heliyon*, 7(3), 2021.

[23] R. K. Gohivar, S. K. Yadav, R. P. Koirala, G. K. Shrestha, and D. Adhikari. Temperature dependence of interaction parameters for Al–Li liquid alloy. *Philosophical Magazine*, 101(2):179–192, 2021.

[24] George Kaptay. A coherent set of model equations for various surface and interface energies in systems with liquid and solid metals and alloys. *Advances in colloid and interface science*, 283:102212, 2020.

[25] Eric Adolph Brandes and G. B. Brook. *Smithells metals reference book*. Elsevier, 2013.